Journal of Structural Geology, Vol. 12, No. 3, pp. 351 to 363, 1990
Printed in Great Britain

0191-8141/90 $03.00+0.00

Experimental calcite fabrics in a synthetic weaker aggregate by coaxial and non-coaxial deformation

G. J. BORRADAILE and J. MCARTHUR

Geology Department, Lakehead University, Thunder Bay, Ontario, Canada P7B 5E1

(*Received* 3 *June* 1989; *accepted in revised form* 12 *November* 1989)

Abstract—Calcite grain aggregates, supported by a weaker, macroscopically ductile, matrix of set Portland cement, were deformed triaxially at room temperature with a confining pressure of 150 MPa and at rates corresponding to a pure shear, natural strain rate of 10^{-5} s^{-1}. Extensive grain rotation accompanied the twinning of calcite. Stress orientations inside the specimens, determined from calcite twins, agree well with the stresses imposed upon the specimens. Thus calcite twins are sound kinematic indicators in this study. Various sample configurations were used to simulate pure shear, transpression and simple shear. In pure shear or coaxial strain, preferred dimensional orientations (*PDO*) of calcite are produced more efficiently in the presence of high pore fluid pressure. Those grain alignments are stronger than the bulk strain would predict assuming homogeneous strain. Strain is overestimated by methods assuming continuum behaviour because they fail to take into account the extensive interparticle motions that occur in the presence of high pore fluid pressure. Fluid pressure suppresses the twinning of calcite by reducing the intergranular stresses. During deformation, small rapid variations in pore fluid pressure are believed to represent ephemeral dilatations accompanying particulate flow as groups of grains slide past one another.

In dry specimens, pure shear is more effective than simple shear in producing a *PDO* of the calcite grains. Calcite grains are rotated rigidly and somewhat strained to produce $L < S$ alignment fabrics in pure shear but give *S*-fabrics in transpression and perhaps also in simple shear. Thus grain-shape fabrics do not conform to the symmetry of bulk deformation in this study. Mean grain alignment is perpendicular to shortening in pure shear, initially inclined and later parallel to shear zone walls in transpression, and weak but statistically inclined to shear zone walls in simple shear. The mean orientation of grain-alignment fabrics is therefore a reliable kinematic indicator under the conditions investigated.

At comparable strains in dry tests, *e*-twinning is best developed in transpression, next best developed in coaxial strain and least well shown by simple shear. High fluid pressure considerably reduces the incidence of twinning.

INTRODUCTION

CALCITE deforms easily by geologically realistic mechanisms in the laboratory. This permits investigation of aspects of the three-dimensional response of a monomineralic polycrystal to deformation. Most previous studies have concentrated on intra-granular effects by studying single crystals or marbles with tightly packed grains.

The goals of this work are to complement existing studies by deforming matrix-supported calcite that is permitted to spin in a somewhat weaker, fine-grained matrix. In this way, we may study the effects of grain alignment and interparticle motions as they accompany grain deformation. Our tests reproduce pure shear, with and without externally applied pore fluid pressures, and also simple shear and transpressive shear.

The medium we chose to deform produces fabrics that are homogeneous at the thin-section scale, being free from differentiations or recrystallization effects such as were produced in comparable studies by Friedman & Higgs (1981) and Jordan (1987). It is not the intention of this paper to reproduce the high-strain kinematic indicators of porphyroclastic rocks such as delta-structures or sigma-structures described by Passchier & Simpson (1986). Such features develop usually with bulk shear strains >2, whereas our strains are lower. Comparisons with the theoretical predictions of Ghosh & Ramberg (1976) are also difficult because the effects they studied are relevant to rigid markers with higher initial aspect ratios than our calcite, and much higher strains.

The porphyroclasts of calcite in this study undergo deformation as the grains spin as rigid bodies. It will be shown that most of the rotation is of the rigid-body kind although the calcite grains are strained also. Most of our knowledge of calcite deformation comes from studies on marbles. In calcite rocks, Turner (1953, *inter alia*) demonstrated that twinning on *e* (plus *r*-glide) is responsible for developing a preferred crystallographic orientation (*PCO*) as shown by the *c*-axes. Weiss & Turner (1972) subsequently showed that, at low temperatures, twinning, which is grain-size dependent, is easier than translation gliding on *r*. Glide on *r* becomes more important between 400 and 650°C, and *f*-slip dominates between 500 and 800°C (Griggs *et al.* 1960, Casey *et al.* 1978, Friedman & Higgs 1981).

With sufficient confining pressure to suppress cataclasis it is possible to deform a calcite rock at low temperature, by twinning, with small amounts of heterogeneous deformation at grain boundaries to suppress dilation. In experiments on marbles, *r*-glide and *e*-twinning tend to rotate *e*-twin planes to an orientation normal to the compression direction so that an *e*-pole maximum develops parallel to the compression axis. Since the *c*-axis is 26° from the *e*-pole, this means that a broad maximum or small girdle of *c*-axes may result from a uniaxial

compression. This has been confirmed experimentally (e.g. Turner *et al.* 1956, Rutter & Rusbridge 1977) and has been successfully modelled assuming that the preferred crystallographic orientation (*PCO*) develops largely by *e*-twinning at low temperatures and largely by *r*-glide at higher temperatures (Casey *et al.* 1978, Wenk *et al.* 1986b).

Natural deformation of calcite rocks usually produces a broad *c*-axis maximum that is approximately perpendicular to the elongate shape of the calcite grains (e.g. Dietrich & Song 1984). However, the twinning recognizable in metamorphic calcite rocks is often asymmetric with respect to the regional flattening deformation or is otherwise considered to post-date the preferred dimensional orientation (*PDO*) fabric of the calcite (e.g. Turner 1953, Dietrich & Song 1984). Early non-coaxial experiments on calcite rocks (Rutter & Rusbridge 1977) used a two-stage shortening of the same specimen in different directions. They showed that in marble the *PCO* rotated more quickly than the *PDO*. Previous experimental work on calcite rocks used natural limestones or marbles as starting materials. In those cases the amount of rotation of the grains is considerably limited by the constraints placed upon each grain by its neighbours. The low strains (usually <30%) achieved by coaxial shortening produce relatively little rotation of the grains in these circumstances and a shortening of 17% achieved the maximum *PCO* in Owens & Rutter's (1978) experiments. In this study, the calcite aggregates have been synthesized by mixing calcite fragments of a uniform grain size with commercial Portland cement. This relatively soft matrix permits almost unrestrained rigid-body rotation and alignment of the grains while they twin and deform at the same time, with relatively low bulk strains of up to 35% axial shortening. Our synthetic material is in some ways a better analogue to the early deformation history of natural rocks in which certain porphyroclasts or porphyroblasts in a rock deform plastically while spinning in a softer matrix. The calcite grains deform incompletely by twinning on thin, closely-spaced twin lamellae, typical of low-temperature deformation. They align primarily by rigid-body rotation. The deformation of the cement matrix is poorly understood. Our observations suggest that the collapse of pore space and micro-cataclasis are important mechanisms. However, the possibility of plastic deformation of cement crystals and some contribution by water during the progressive phase changes in hardening cement cannot be ruled out.

EXPERIMENTAL PROCEDURES

The synthetic material was produced by mixing volumes of 60% mineral grains with 40% dry cement powder and then wetting the mixture to set the cement. The calcite mineral grains had been derived by crushing vein-calcite and then sieving this to the grain size range of 0.176–0.25 mm. After setting for 28 days, cores 20 mm in diameter were drilled from this block of material and prepared as right-cylinders about 25 mm long. These specimens were used for the axial-symmetrical shortening experiments or *coaxial tests* that simulated pure shear. Specimens were air-dried for at least 2 weeks before testing. However, cement retains free water which is progressively taken up by hydration reactions as cement ages. For this reason, all 'dry tests' involve water in the deformation of the Portland cement matrix. In order to investigate the effects of high fluid pressures, one series of coaxial tests was run with a pore-fluid pressure applied artificially by an external apparatus through the hollow upper piston. Distilled water was used with a fluid pressure (P_f) nominally equal to 95% of the confining pressure (P_c).

Two further experimental assemblies were used to simulate non-coaxial strain histories in air-dried samples. The *transpressive* or oblique-shear assembly, devised by Friedman & Higgs (1981) uses elliptical slices of the material being studied, inserted into cylinders of stiff sandstone. In our tests the slices were inserted along a pre-cut direction making 55° with the cylinder long axis. These discs were ground to a thickness of approximately 4 mm and inserted into pre-cut cylinders of hard quartz–sandstone to provide a shear-type of environment for the calcite aggregate (Fig. 1b). The specimens were jacketed in Teflon tubes with back-up jackets of heat-shrink tubing to ensure a good seal. The previous studies using this arrangement used a pre-cut angle of 35°. Our arrangement was chosen, initially, so that the elliptical discs would not have such a high aspect ratio, thereby facilitating measurements of the magnetic susceptibility (see Borradaile & Alford 1988). However, an advantage of our arrangement is that it produces a stronger component of transpression. The shear strains produced for a given shortening of the cylinder are also smaller, although the shear stresses along the pre-cut direction are the same as in the 35° pre-cut arrangement of Friedman & Higgs.

The *simple shear* assembly used to produce non-coaxial strain histories was devised for studying fault

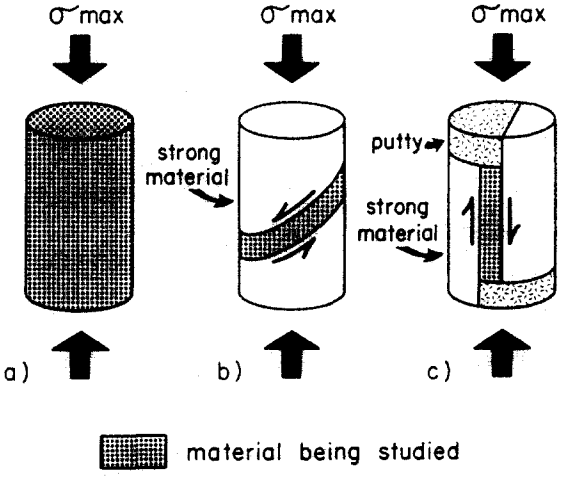

Fig. 1. Sample assemblies of the synthetic material being investigated in the various arrangements. Left: to produce coaxial strain (approximately pure shear). Middle: to produce transpressive shear (oblique assembly). Right: to produce simple shear (longitudinal assembly).

gouge (John Logan personal communication 1988). It is illustrated in Fig. 1(c). In this case a longitudinal pre-cut is made in the stiff sandstone cylinder and a 2 or 4 mm thick rectangular slice of the synthetic material is inserted into it. The stiff sandstone pieces are offset at the ends and the gaps are filled with putty. In this arrangement the normal stress acting across the shear zone is constant and equal to the confining pressure. As long as the assembly is not shortened beyond the limit set by the compaction of the putty, the deformation of the inserted slice of synthetic material is not transpressive and closely approximates simple shear. There were only very small decreases (<1%) in thickness of the shear zones in the latter type of assembly, confirming a close approximation to simple shear.

The specimens were deformed at a confining pressure (P_c = minimum stress) at either 150 or 200 MPa in a Donath triaxial rig. Loading was provided by a multi-geared syringe pump that was controlled by an IBM personal computer with a Taurus analogue-digital converter (12-bit) system. The axial stress, piston displacement, confining pressure and pore-fluid pressure were monitored electronically. This permitted the computer program to perform the data reduction (corrections for apparatus distortion, etc.) during the test and to control automatically the rate of loading via an analog output to produce a truly constant (natural) strain rate. The rate used was 5×10^{-6} or 1×10^{-5} s^{-1} for the axial shortening experiments, with an error of <3% in any 5 min period. For the shear experiments, the pistons were advanced at a constant displacement rate (as opposed to the non-linearly decreasing rate of the constant *strain* rate tests) to produce a slip rate of 0.73×10^{-4} mm s^{-1} on the walls of the shear zones where the slice was initially about 4 mm thick. This slip-rate increased slightly during the start of the oblique-shear tests as the shear-disc compacted. In the oblique shear tests the maximum shear strain achieved was about 0.19 before transpressive compaction (parallel to the axis of the cylindrical assembly) dominated the deformation history. In the longitudinal shear zone tests larger shear strains ($\gamma < 0.5$ for 4 mm thick slices and <1.0 for 2 mm thick slices) were possible before transpression occurred (beyond a γ value = 0.5): the use of thinner shear-slices increased the shear strain further.

There are no differences observed between the results obtained at the two different confining pressures or for the pure shear tests performed at the two different strain rates.

Deformed specimens were impregnated with araldite and sectioned parallel to the axis of the cylindrical specimen and perpendicular to this direction. In the case of the shear zone assembly specimens, sections were made perpendicular to the sheared disc in directions that were perpendicular and parallel to the shear direction in the disc. These perpendicular pairs of thin sections made it easier for complete *c*-axis patterns to be determined by a four-axis Universal stage. Between 50 and 100 grains were used for twin and *c*-axis studies. Photographs of the thin sections were digitized using a Zeiss-Kontron image analysis system. This permitted consistent, automatic fabric and strain analysis (by Robin's method, 1977) using between 200 and 400 grains per sample.

Initial fabrics

The starting material was carefully mixed to avoid producing strong grain alignments or 'flowage' dimensional fabrics of the calcite. Our studies of digitized photographs lead us to believe that no significant preferred dimensional orientations (*PDO*) are present in the starting material (see Fig. 8a). This was advantageous as it permitted us to use Robin's method of strain analysis, rather than an R_f/ϕ method. This greatly reduces the ambiguity of the strain analyses of the deformed synthetic aggregate. Crystallographic fabrics in the deformed material are studied using *c*-axes and *e*-twins. Moreover, compression directions responsible for twinning are determined from a combination of *c*-axes and *e*-twins for the same grain, supplemented by information on the spacing of the *e*-lamellae. Consequently we also investigated the crystal fabrics of the starting material. Some twinning is present, due to sample preparation, but as expected this is randomly oriented in the starting material (Fig. 2a). Even after the application of hydrostatic confining pressure of 200 MPa (which preceded each test) there is only a slight increase in the intensity of twinning (as shown by the spacing of lamellae per mm), but no preferred orientation (Fig. 2b). Thus we are confident that our starting material is free from any *PCO* or *PDO*.

The effects of the Portland cement

The properties of Portland cement and its deformation mechanisms under high confining pressures are not well understood. In coaxial tests the cement rapidly compacts early in the test. The initial volume occupied by mineral grains is about 50% and this increases to about 68% after 22% axial compression. Compaction is

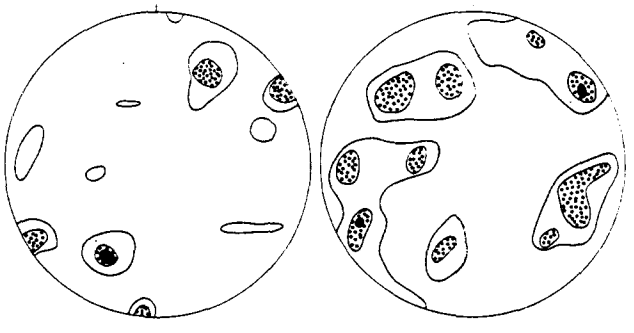

Fig. 2. Crystallographic fabrics in the synthetic aggregate used for the experiments. (a) After cement has set, prior to any test. (b) Hydrostatic test: after compaction at 200 MPa, but prior to any differential stress. The diagrams contour the spacing of *e*-twin lamellae at the position of the compression direction inferred for that twin orientation by Turner's method. Consequently most of this twinning is attributed to sample preparation, prior to mixing the aggregate.

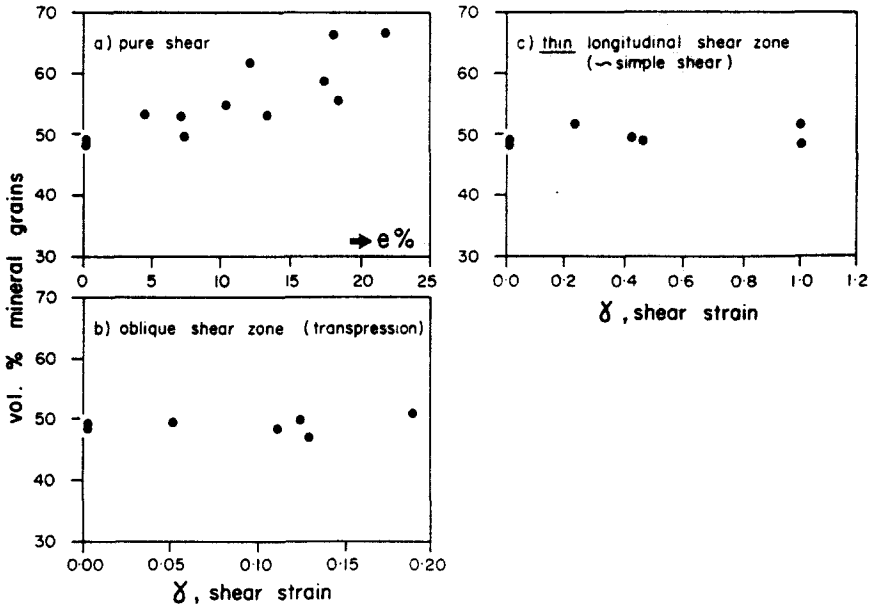

Fig. 3. Compaction of cement matrix in the three types of dry test. Only coaxial strain (pure shear) produced marked compaction. Compaction is even more marked for coaxial strain in the presence of a high pore pressure, see Fig. 11.

not detectable to the same extent in the transpressive tests and is practically absent in the simple shear tests (see Fig. 3). In all types of test some microscopic evidence of compaction is found. The pores of the cement are rapidly collapsed and the delicate crystal forms are replaced by more amorphous grain shapes after a few percent strain. This is attributed to microcataclasis and is shown in the scanning electron microscope pictures of Figs. 4(a) & (b).

The permeability of the cement–calcite aggregate decreases early in the tests as small bubbles collapse. Those near the surface of the specimen were filled with cement or putty prior to testing but this did not always prevent the jacket from failure. When the jacket is perforated early in a test, at less than 4% axial shortening of a solid cylindrical specimen, there can be a catastrophic loss of confining pressure fluid through the specimen to the atmosphere through a vent in the upper stationary 'piston' of the pressure vessel. In contrast, if the jacket fails at a later stage in the test there is no noticeable loss of confining pressure apart from the initial slight and gradual decrease due to compaction. Instead the specimen decreases in strength gradually as it becomes saturated with oil. In previous work (Borradaile & Alford 1987, fig. 14) an anomalously strong magnetic fabric developed in a specimen which deformed with the accidental introduction of pore fluid at a late stage in the test. Thus we have investigated the effects of pore fluid pressure.

Pore fluid pressure effects in coaxial tests. Although the cement always contains some free water, we deliberately applied fluid pressure to some coaxially deformed samples. Complete wetting of the samples confirmed that the distilled water penetrated the material. As expected, fluid pressure reduces the flow strength of the samples considerably (Fig. 6). Dry flow strength, the 'steady state' strength, is ≥200 MPa, but a constant pore fluid pressure (P_f) equal to 95% of the confining pressure reduces this to about 70 MPa. The flow strength may be reduced further by increasing the fluid pressure in steps separated by pauses (points connected by tie-lines in Fig. 6). In one test the jacket was deliberately ruptured and the pore fluid pressure was equalized with the confining pressure: this reduced the flow strength to <10 MPa.

Clearly, pore pressure has a great effect on reducing flow strength and the pulsations of pore pressure and differential stress are believed to be due to ephemeral dilations as groups of grains slide past one another (Fig. 7). This process has previously been called particulate flow (Borradaile 1981).

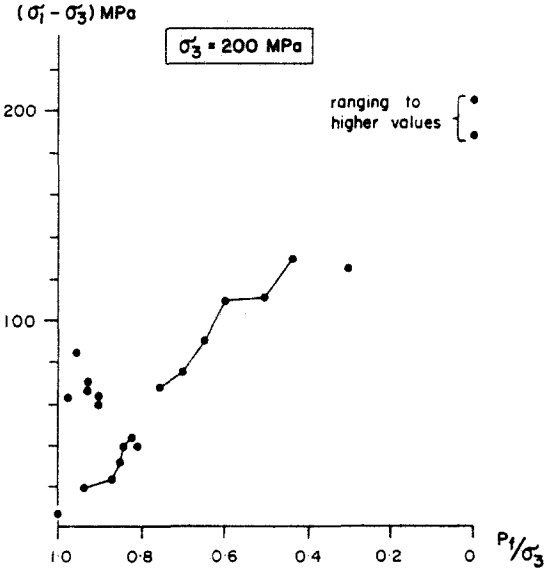

Fig. 6. The effects of pore fluid pressure (P_f) on flow strength. Dry specimens have flow strengths >200 MPa. The 'flow strength' is the estimate of the steady-state flow stress. This is reduced to about 70 MPa when P_f is 95% of the confining pressure. Strength is reduced further if P_f is increased in steps with pauses in between (those data points are connected by tie lines).

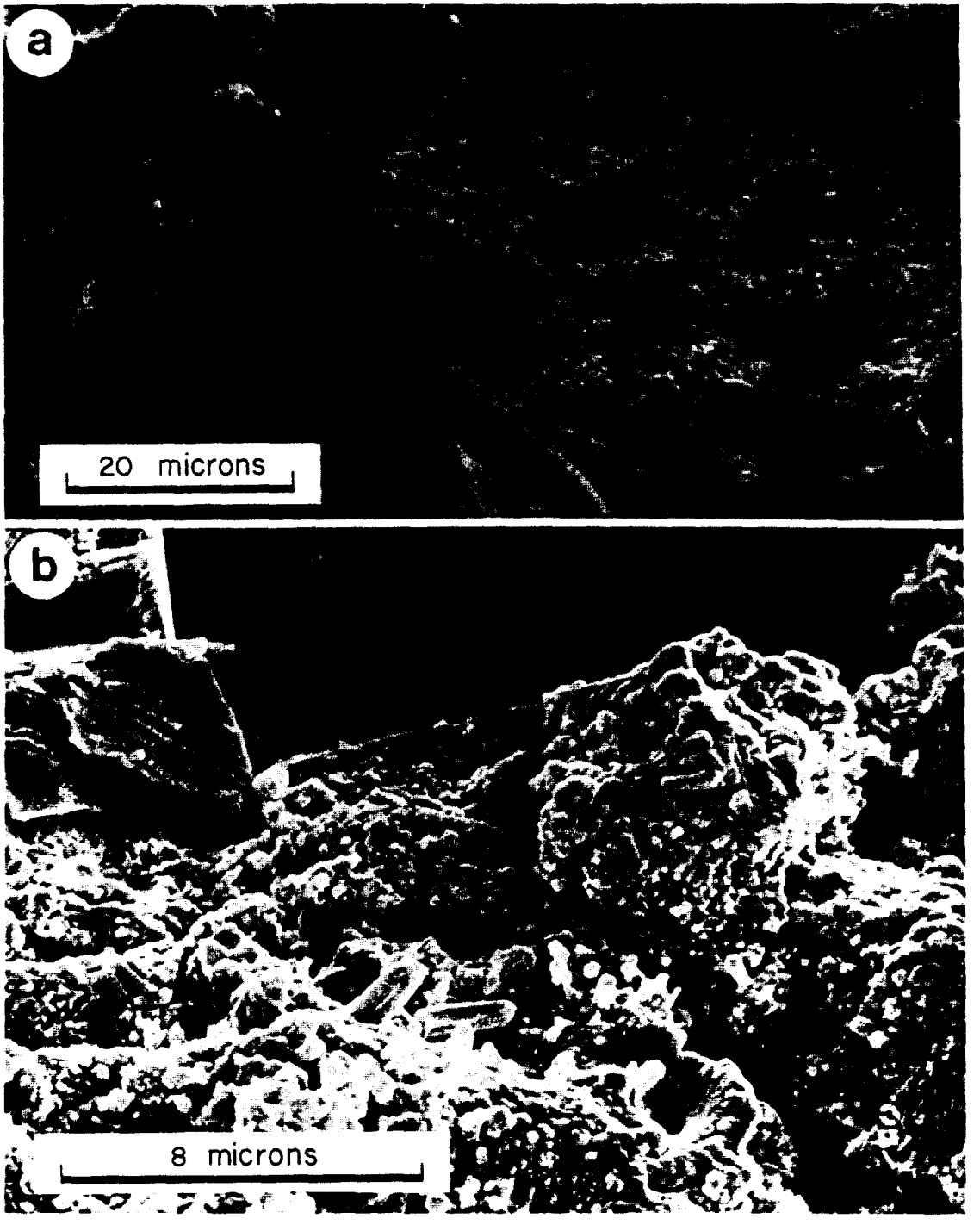

Fig. 4. Scanning electron micrographs of the Portland-cemented calcite aggregates (a) before and (b) after 5% coaxial deformation. (a) Note the delicate crystalline nature of the cement between the two calcite grains. (b) After a small deformation the cement loses much of its crystalline detail and is more compact.

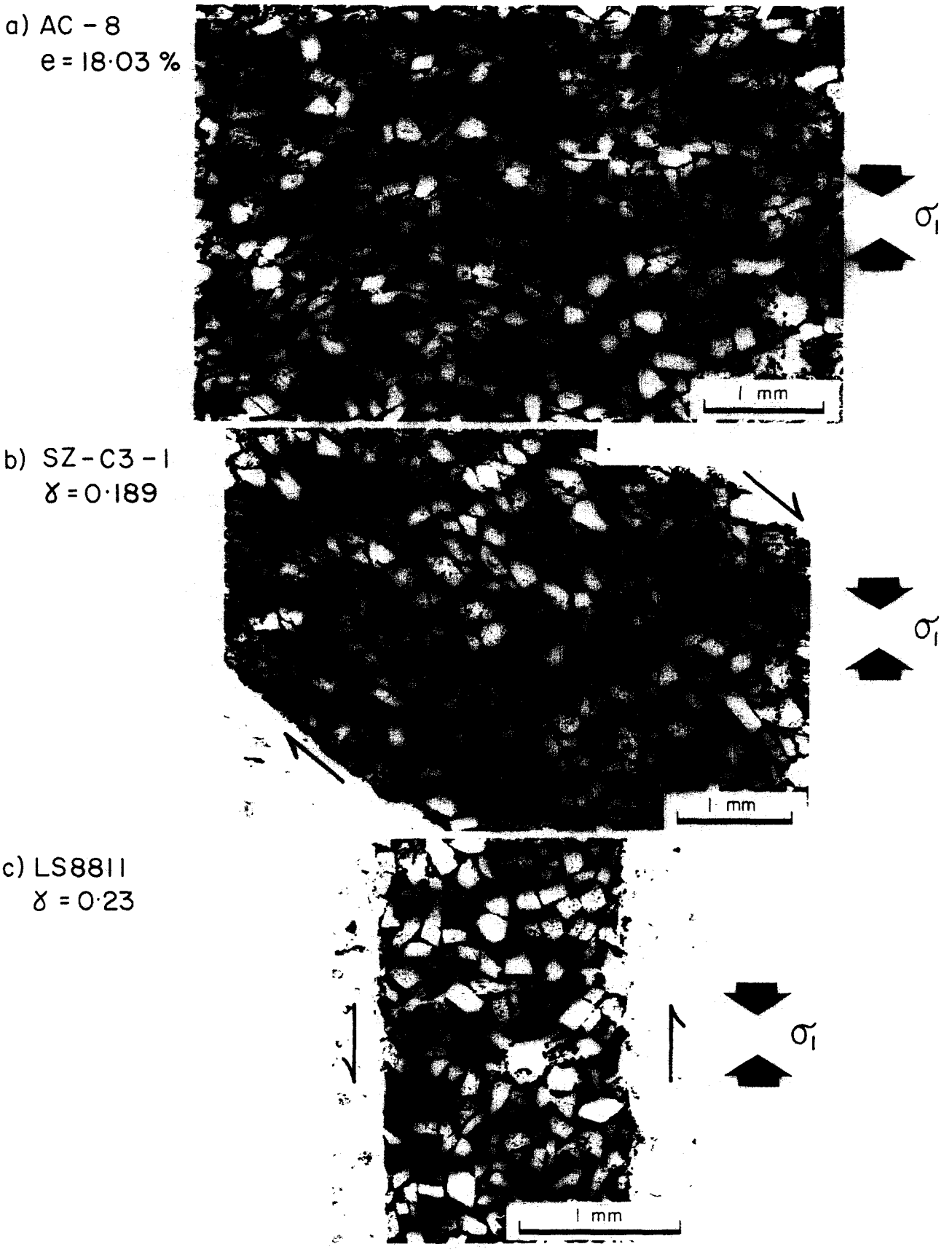

Fig. 5. Photomicrographs of the Portland-cemented calcite aggregates after (a) coaxial strain, (b) transpressive shear and (c) simple shear. Twinning is developed in all cases as the result of experimental deformation but preferred dimensional orientations are only recognizable in the coaxial and transpressive tests shown here (b & c). Borradaile & Alford (1988, fig. 5b) show an example of a transpressive test in which an oblique fabric has developed due to a lower shear strain than that shown in (b).

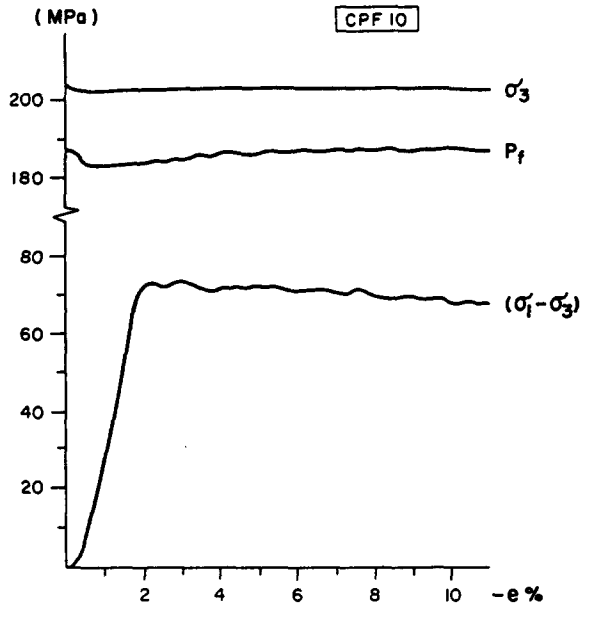

Fig. 7. Stress–strain, P_f and confining pressure variations during a test in which a pore fluid pressure (using water) was applied to the specimen. Note the oscillation of P_f and differential stress $(\sigma_1 - \sigma_3)$ during flow. In some tests this effect was so great that the confining pressure also oscillated sluggishly.

RESULTS

(A) *Coaxial tests* (*dry*; $P_f = 0$)

Preferred dimensional orientation (PDO). Data are presented on R_f/ϕ diagrams (Fig. 8) which indicate the tendency of the grains to align in a direction perpendicular to the compression direction. This fabric is also illustrated in Fig. 5(a) (18% strain) and becomes very noticeable beyond 20% strain.

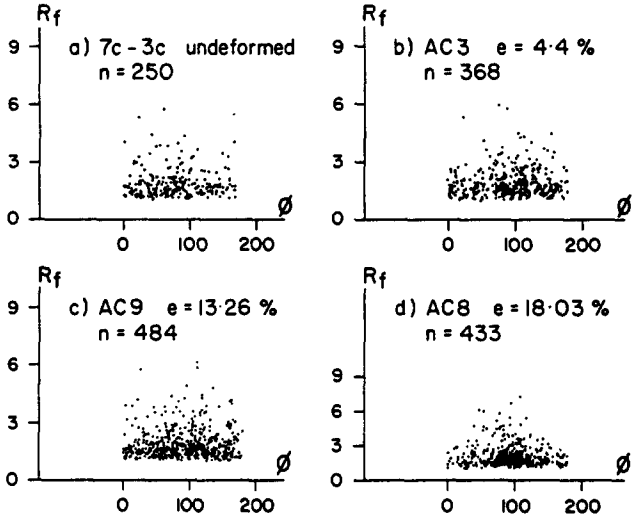

Fig. 8. Preferred dimensional orientation of calcite grains after coaxial strain (pure shear) of the samples. The axial ratios (R_f) are plotted against the orientation (ϕ) of the grains' long axes with respect to the plane of flattening. The ϕ axis has a 180° range and the flattening direction is located at 90° for (b), (c) & (d). No preferred orientation is evident in the undeformed specimen (a), but a slight preferred orientation is evident even at 4.4% strain and is well developed at 18% strain. In all cases, however, even up to 34% shortening, the range of ϕ is 180°.

PDO starts to develop at quite low strains (4%) and is pronounced at 18%. Nevertheless, the fluctuation of long axes of grains (ϕ) is 180° in all cases. The relatively strong alignments occur because the calcite grains rotate rigidly through the cement matrix. The *PDO* is believed to be mainly due to rigid rotation, because the grains can only deform internally to a limited degree and because of the relatively strong alignments of the long axes of grains with low axial ratios.

Preferred crystallographic orientation (PCO). Calcite *PCO* changes rapidly, even in the first few per cent of deformation. The undeformed specimens show no *PCO* as detected from *c*-axes, *e*-twin lamellae or from the lamellae index spacing, which is the number of lamellae per mm when the lamellae are viewed edge-wise with the U-stage. Data are presented for specimens shortened 4% and 18% (Figs. 9 and 10). These show significant increases in the intensity of twinning, as shown by the average number of *e*-lamellae per mm (Fig. 22).

The twins may be used to infer the principal stresses inside the samples using Turner's method. Although the results are not unexpected for the coaxial tests, in subsequent non-coaxial experiments the external stress system imposed by the triaxial rig may not be directly relevant inside the specimen.

Turner's (1953) method of determining the principal compressive stress direction from individual grains is commonly used. It is a simple geometrical construction based on the assumption that the best-developed set of twin lamella is in the optimum orientation for shearing. Since this is not universally true, the method produces some spurious results but this is well known and the

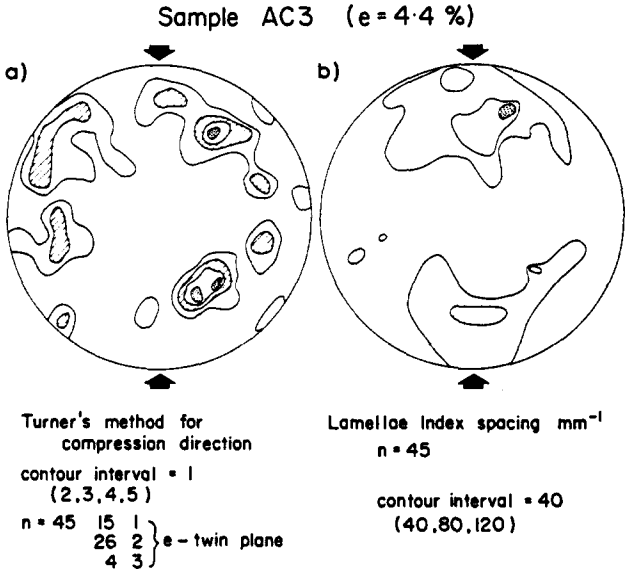

Fig. 9. Preferred crystallographic orientation (*PCO*) in a specimen shortened by 4.4% by pure shear. The compression direction of the triaxial rig is shown by the black arrows. (a) Turner's (1953) method for determining the compression directions of individual twinned grains gives some spurious data points as is well known. (b) The spacing of the twin lamellae is contoured for each of the compression directions in Fig. 8(d). This filters out spurious data, so that the remaining compression directions agree fairly closely with the loading axis of the triaxial rig.

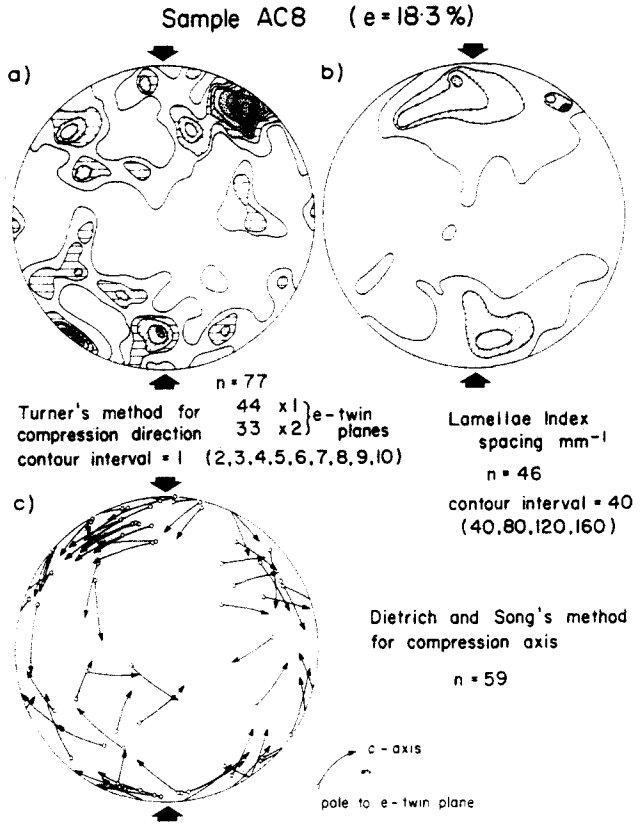

Fig. 10. Preferred crystallographic orientation in a specimen shortened by 18% in pure shear. The black arrows give the shortening axis of the experimentally deformed specimens. (a) Turner's (1953) method gives spurious results for the compression directions, even with 77 grains. (b) The contours of the spacing of *e*-lamellae, recommended here, more faithfully emphasizes the axial compression direction of the specimen, despite the small number of data ($n = 46$ grains). (c) Dietrich & Song's (1984) method for determining the compression direction from the *PCO* is not very successful here, probably because the strain is too low. Nevertheless, some systematic pattern does emerge with *e*-poles located closer to the compression direction than the host *c*-axis orientation.

technique is still useful where the strain is large and where the grains are restricted from large rigid-body rotations as in marbles. In the low-strain experiments the technique is less useful. The spurious nature of compression directions is shown (Fig. 9a) for 4% shortening. However, Turner & Ch'ih (1951) noted that the most favourably oriented crystals showed the highest frequency of *e*-twin lamella. Friedman & Conger (1964) filtered out most of the spurious data by omitting twins from the diagram that had <60 lamellae per mm. We extended this notion by recording the lamellae spacing index for every twin-set measured on the stereonet, at the position of the compression direction inferred by Turner's method. These data were then contoured: the maxima are found to give a good indication of the external compression axis (Fig. 9b), which in our case is known. The benefits of this technique are greatest with the numerous, low-temperature twins and modest bulk strains that our experiments have produced. However, the large rigid-body rotations of the grains, especially strongly deformed grains, can shift the inferred compression directions.

At 18% strain Turner's method (Fig. 10a) provides a slightly better estimate of the externally imposed stresses but contouring the lamellae spacing is more accurate (Fig. 10b). The strain is still not high enough to utilize Dietrich & Song's (1984) improvement of the Turner method (Fig. 10c) which is more applicable in field studies of highly strained rocks. Nevertheless, the *e*-poles congregate around the compressive stress direction and the *c*-axes make small angles with it. Contours of lamellae frequency require fewer grains and therefore seem to provide the most appropriate method to locate compression directions. This is advantageous in studying non-coaxially deformed specimens at these low shear strains because they are small in volume and yield few grains for measurement. It may also be recommended for field studies where low-temperature twinning and modest strains are involved.

(B) *Coaxial tests* (*wet*; $P_f > 0.9\ P_c$)

Preferred dimensional orientation (PDO). The cement matrix compacts more readily in wet tests (Fig. 11) than dry tests (Fig. 3a). The alignment of calcite grains increases rapidly and is more complete in wet tests. This is shown by the reduction in the standard deviation of angular dispersion of long axes (ϕ) with strain (Fig. 12a). This is significantly faster than in dry tests (Fig. 20a). Similarly to the dry tests (Fig. 20), textures are produced in which there is a slight tendency for $S > L$ fabrics to develop (Fig. 12b). However, the progression of mean grain shapes across the Flinn diagram (the 'deformation path') is more regular in the wet tests.

Preferred crystallographic orientation (PCO). Wet tests also produce differences in calcite *PCO*. The intensity of twinning is, on average, 20% less than in dry tests at the same strain (see Fig. 22). This is attributed to lower intergranular stresses in the presence of high P_f. However, the grains are much better aligned with their *e*-twin poles aligned close to parallelism with the loading axis. This is shown in Fig. 13 by the compression directions for individual grains (as determined by Turner's method and contoured by the intensity of twinning). The individual compression directions have a maximum fre-

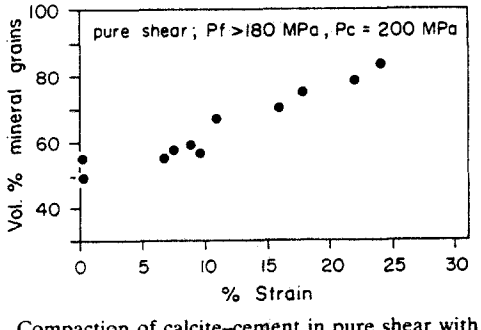

Fig. 11. Compaction of calcite-cement in pure shear with high pore fluid pressures ($P_f > 0.9\ P_c$). Note that the compaction of the cement is about 10% greater than in dry tests at 20% strain (cf. Fig. 3a).

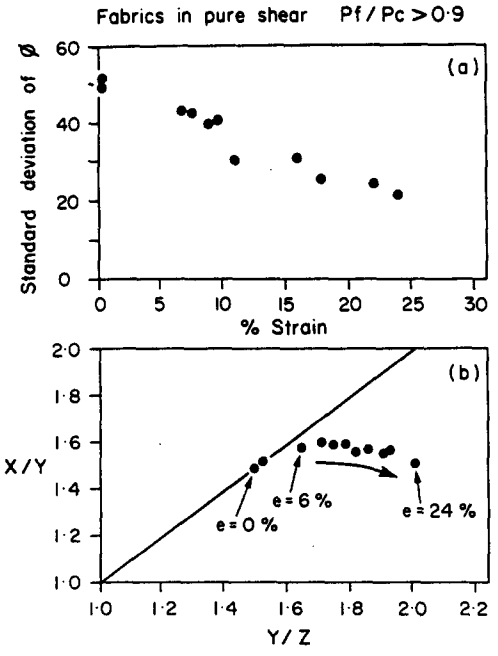

Fig. 12. Grain-shape development (*PDO*) in high pore fluid pressure coaxial tests. (a) Standard deviation of ϕ (long axis orientation) decreases with strain (more rapidly than in dry tests, see Fig. 20 upper left graph). (b) Grain shapes progress slightly into the flattening or $S > L$ field on the Flinn diagram.

quency of twin-lamellae spacing for the inferred compression directions that are parallel to the experimental loading axis, but there is also a 45° small girdle around the loading axis caused by the very strong alignment of *e*-twin planes (Fig. 13). The combination of reduced twinning but enhanced grain alignment is attributed to rigid-body rotation during particulate flow.

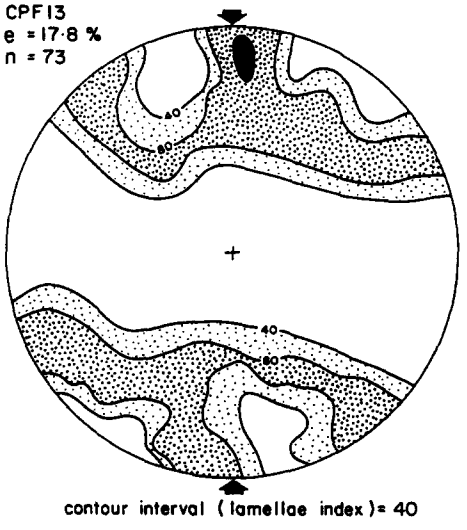

Fig. 13. Preferred crystallographic orientation after pure shear of a specimen with pore fluid pressure at 95% of the confining pressure. The spacing of twin lamellae, contoured at the individual compression axes as determined by Turner's (1953) method, accurately locate the internal principal compressive stress in the N–S direction, parallel to the externally imposed axial load. In this case the preferred orientation of *e*-twin poles in the N–S direction is very strong. This causes the compression axes determined by Turner's construction for individual grains to form a small girdle 45° from the axis of maximum stress.

(C) *Non-coaxial deformation experiments (all dry, $P_f = 0$): transpressive tests*

For the non-coaxial experiments, elliptical discs of the calcite aggregate were placed in pre-cut zones in cylindrical sandstone assemblies such that the discs made an angle of 55° with the cylinder axis (Fig. 1b). The shear discs were usually 4 mm thick and their shear strain rate was approximately 0.55×10^{-4} s^{-1}. This increased slightly through the test as the shear disc compacted and became slightly thinner.

The cylindrical specimen assembly is placed between a fixed upper steel piston and a lower steel 'anvil' that is free to slide laterally during the compression of the cylindrical assembly. Thus bending of steel pistons is avoided and modest shear strains are achieved for quite thick shear zones. The maximum shear strain achieved by this technique is 0.38 for a 4 mm thick shear zone. This is considerably less than the shear strains achieved by others, using the technique of Friedman & Higgs (1981). Higher shear strains were produced by others because their shear zones were very thin and at an angle of 35° to the axial shortening direction.

Preferred dimensional orientation. In oblique shear zone tests *PDO* develops rapidly in comparison with the dry, coaxial tests. Figures 14 (a) & (b) present R_f/ϕ data for two tests with small shear strains of 0.111 and 0.189 (the shortening associated with the same strain ratio in pure shear would be less than 10%). Nevertheless, the R_f/ϕ diagrams show marked *PDO* development and this soon (for example, by a shear strain of 0.189) rotates into parallelism with the boundaries of the shear zone.

*Preferred crystallographic orientation. PCO*s develop well with little strain in oblique shear zones: effects of successively greater shear strains (0.111, 0.129, 0.189) are shown in Figs. 15–17. At lower shear strains (e.g. 0.111 in Fig. 15b; 0.129 in Fig. 16b) the *e*-poles tend to be closer to an alignment with the compression direction of the triaxial rig (given by the black arrows in the figures). At higher shear strains (e.g. 0.189) the alignments of *c*-axes produced by a combination of *e*-twinning and rigid-body rotation show a tendency to be perpendicular to the shear zone (Fig. 17b). At the highest shear strain, still quite modest by comparison with the strains usually studied in natural rocks, Dietrich & Song's method was successfully applied and indicated compression midway between the axial compression of the specimen and compression perpendicular to the shear zone (Fig. 17c). The *c*-axes are expected to rotate in a sense compatible with the shear sense of the shear zone. Most of the examples reported by Schmid *et al.* (1987), and by Friedman & Higgs (1981) confirmed this and the few grains that tended to twin over in a direction perpendicular to the shear zone, or against the sense of shear, were attributed to localized heterogeneous grain deformation (Schmid *et al.* 1987, p. 756). However, in some of our examples (Fig. 17c) many grains twinned in a sense

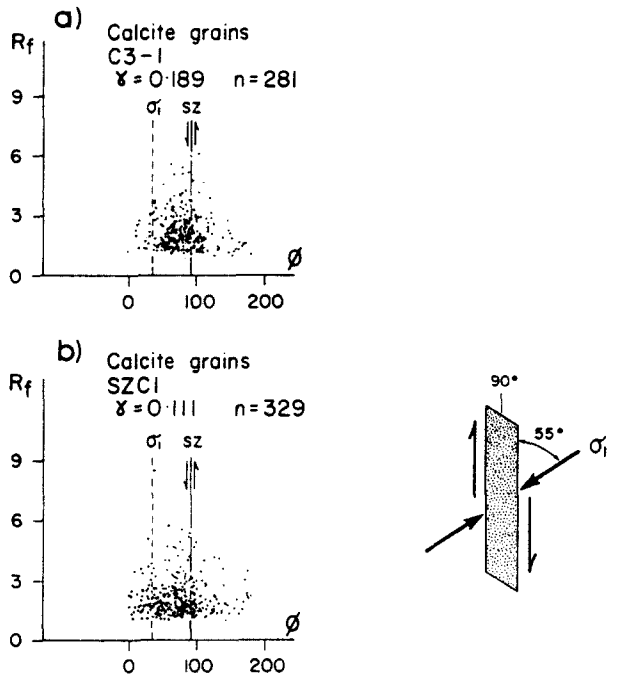

Fig. 14. Preferred dimensional orientation (*PDO*) in calcite grains subject to non-coaxial deformation in an oblique shear zone. Attitude of the shear zone and loading axis of the triaxial rig are shown in inset. R_f/ϕ diagrams correspond with the orientation of compression axis of the rig and attitude of shear zone (SZ). *PDO* of calcite develops early, at a shear strain of only 0.111 (b) and is well developed at 0.189 (a).

(shown by the arrows joining the *e*-pole to the *c*-axis) that is incompatible with the sense of shear zone. Since our grains and the large grains in Friedman & Higgs' experiments are cushioned by a more ductile matrix, this is less likely due to complex grain interactions caused by incompatible plastic deformation of neighbouring grains. It may indicate that the compressional component (parallel to the axis of the cylindrical assembly) is overprinting the shear effects of the transpressional zone. In any case, the calcite's deformation departs

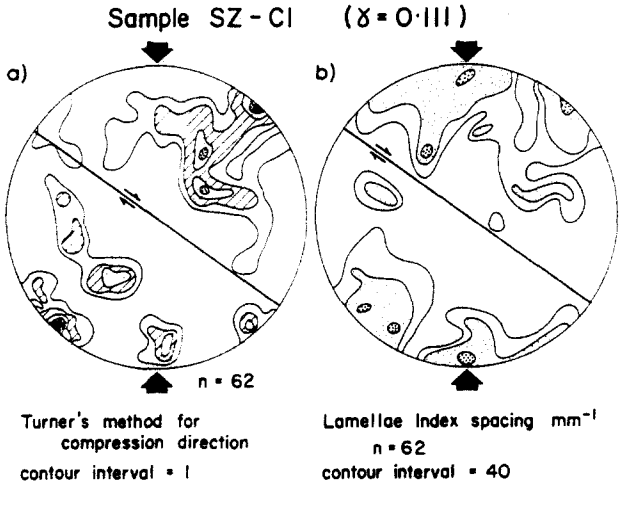

Fig. 15. Preferred crystallographic orientation of calcite yields estimates of principal compression direction in transpressive (oblique shear) tests. Shear strain 0.111: actual axial compression direction of rig shown by heavy arrows. (a) Turner's method, (b) Turner's compression direction contoured in terms of the twin-lamellae spacing, as recommended here.

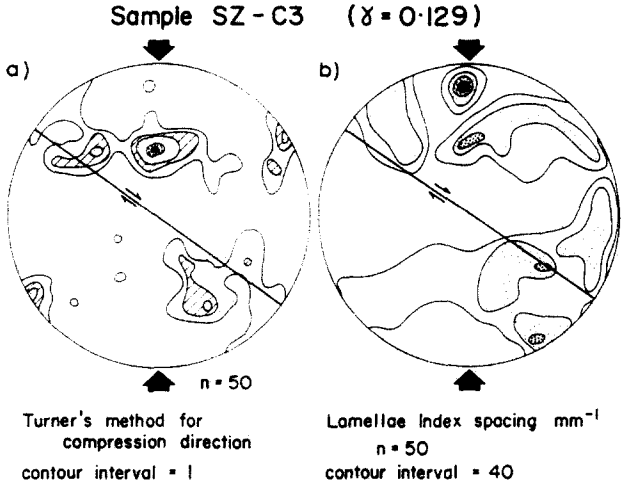

Fig. 16. Estimates of principal compression direction in oblique shear tests at $\gamma = 0.129$. actual axial compression direction of rig shown by heavy arrows. (a) & (b) As in Fig. 15.

considerably from plane strain though not necessarily for the same reasons discovered in the study of Schmid *et al.* (1987, p. 756).

A general problem with the oblique shear zone tests is that a limit is soon reached beyond which the shearing component is subordinate to axial compression of the specimen assembly. Thus all oblique shear zone tests are essentially transpressive, especially beyond shear strains of about 0.4. Moreover, the technique gives rather low shear strains for solid wafers such as we have used.

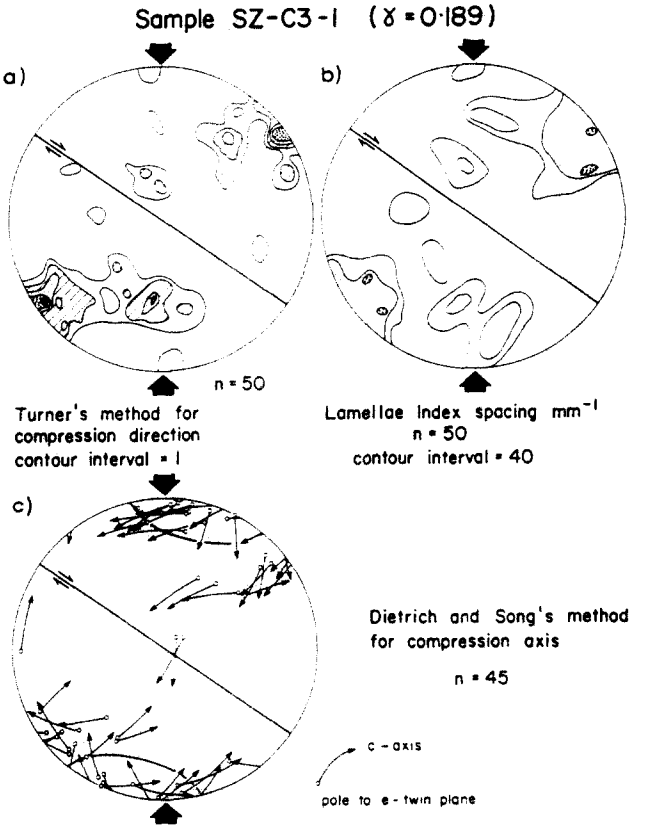

Fig. 17. Estimates of principal compression direction in oblique shear tests at $\gamma = 0.189$, actual axial compression direction shown by heavy arrows. (a) & (b) As in Fig. 15. (c) Dietrich & Song's (1984) method.

(D) *Simple shear tests*

In these tests, a rectangular wafer of the material being studied is inserted along a cut parallel to the axis of a stiffer, cylindrical sample (Fig. 1c). In this arrangement, the normal stress across the wafer remains constant and equal to the confining pressure. This matches simple shear much more closely than the oblique shear zone tests. Shear occurs as the putty compacts and permits the sandstone semi-cylinders to slide past one another. It is difficult to obtain large shear strains because large offsets of the half-cylinders induce tilting of the assembly. The ultimate shear strain is limited by the amount of compaction of the putty and by its extrusion between the assembly and the Teflon jacket. Initially, shear zones 5 mm thick were used but it was found that at larger shear strains the wafer ceased to shear and became shortened in the axial direction. This induced transpression, albeit in a different direction from that produced in the oblique shear zone tests. Later, thinner wafers (2 mm thick) were used and these permitted slightly greater shear strains for the same small displacements of the ends of the half-cylinders.

Preferred dimensional orientation. Deformation produces a very weak alignment (Fig. 5c) or *PDO* of calcite grains, inclined to the shear zone wall, with statistically defineable preferred orientations close to that predicted by the theory of simple shear (Fig. 18b). The fabrics are weaker than in transpressive tests at similar strains. One is tempted to attribute this to slippage between the specimen wafer and the sandstone half-cylinders. However, this is not believed to be the only cause or even a very significant cause, because the asperities of the sandstone indent the calcite–cement wafer and do not show evidence of slippage (Fig. 5c). In contrast, in transpressive oblique shear zones, a strong *PDO* fabric is initially inclined to the zone walls (e.g. see Borradaile & Alford 1988) but aligns rapidly with the walls (Figs. 5b and 18b). In coaxial tests the alignment is simply parallel to the minimum stress (Figs. 5a and 18a).

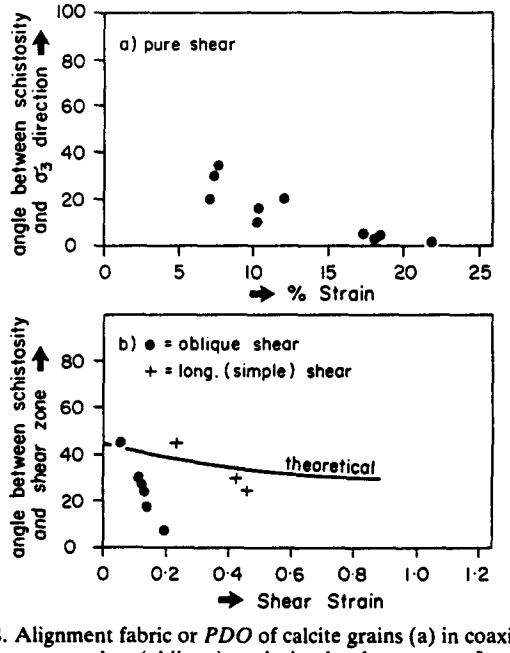

Fig. 18. Alignment fabric or *PDO* of calcite grains (a) in coaxial, and (b) in transpressive (oblique) and simple shear tests. In (b) the theoretical curve for simple shear is shown.

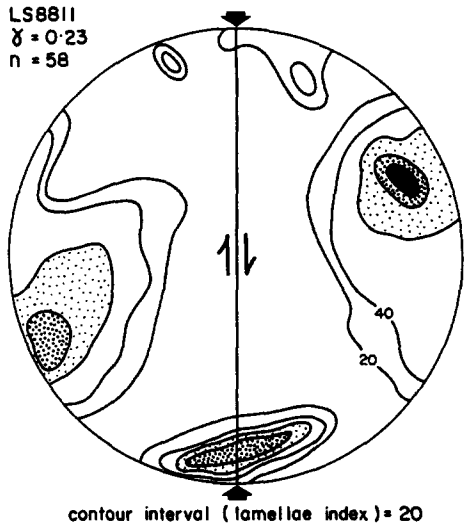

Fig. 19. Preferred crystallographic orientation in calcite in a simple shear zone. Contours of lamellae frequency, described in the text, predict maximum compressive stress in an orientation that is kinematically compatible with simple shear. Externally imposed maximum compressive stress is N–S.

Preferred crystallographic orientation. The modest thinning of the longitudinal shear zones permits a stress regime to develop that is fairly close to that predicted for simple shear. This is shown by the inclination of the internal principal compressive stress to the shear zone walls in a kinematically compatible sense (Fig. 19). This is not modified by rigid-body rotation to any great extent. If tests are continued beyond this stage, axial compression of the assembly dominates over simple shear and transpression occurs. This transpression has a different symmetry from that in the oblique shear zone tests as the compressive component is now parallel to the shear slice.

Generally, the frequency and intensity of twinning is quite low, and is almost comparable to the hydrostatic test. Thus there has been minor change in grain shape. Possibly as a partial consequence of this fact, there is also little rigid-body rotation and a weak *PDO*.

CONCLUSIONS

(1) Compaction of the cement matrix is achieved more completely in pure shear than in transpression or simple shear (Fig. 3).

(2) Compaction of coaxially strained specimens is more effective in the presence of a high fluid pressure ($P_f/P_c > 0.9$). This is believed to be due to particulate flow enhanced by an effective stress principle (Borradaile 1981). Short-lived dilations of the specimen during particulate flow as calcite grain-asperities and groups of grains slide past one another are believed to be the cause

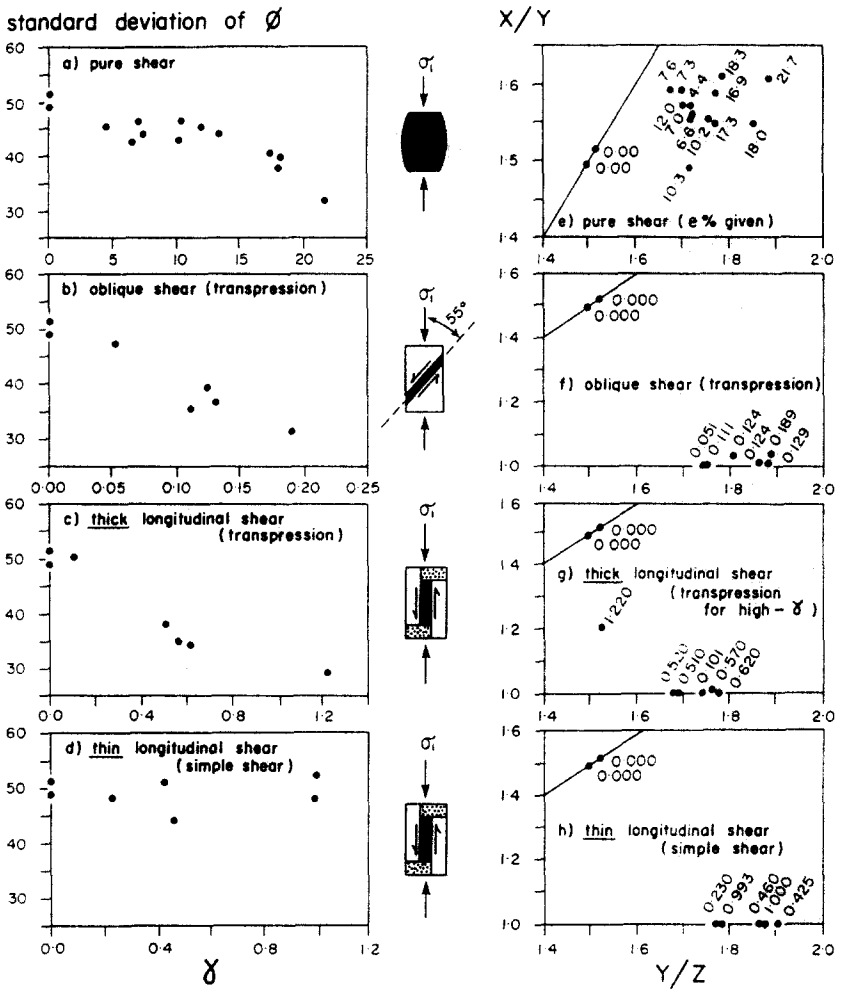

Fig. 20. Comparison of (in left-hand column) fluctuation of ϕ (calcite long axis orientation) and mean grain shape (on Flinn diagrams in right-hand column) for the various geometries of dry tests.

of the fluctuations of pore fluid presure (Fig. 7) during the experiments. Increasing the fluid pressure in stages decreases the strength (Fig. 6) and enhances particulate flow even further.

(3) The effects of particulate flow during high pore fluid pressure in coaxial tests are detectable also from the crystallographic fabrics. Twinning of the calcite is less severe because intragranular stresses are lower: pore fluid pressure supports much of the load.

(4) In coaxial tests, grains are better aligned by deformation in the presence of high pore fluid pressures (cf. Fig. 12a, wet, and 20a, dry). This causes strain analysis methods based on continuum principles to overestimate the strain (Fig. 21). In the high pore fluid pressure tests we believe that the non-continuum process of particulate flow enhances alignment of grains.

(5) In dry tests, coaxial strain (pure shear) and transpressive (oblique) shear produce rapid decreases in the dispersion of grain long axes orientations (ϕ) (see Fig. 20). In simple shear alone, little *PDO* develops.

(6) Calcite grain shapes produced in pure shear strain histories lie just in the $L < S$ field, near the plane strain line of the Flinn diagram (Fig. 20). In contrast, components of simple shear in transpressive tests produce flat or *S*-type grain-shape fabrics. This may also be the case in true simple shear tests, but the weak *PDO* fabrics make it difficult to confirm this. The slight incompatibility of grain shape with deformation is perhaps unexpected. Therefore grain shape could be a somewhat

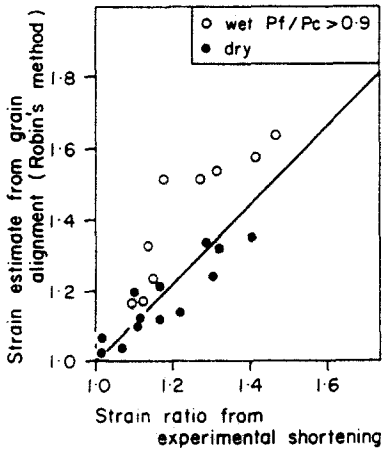

Fig. 21. Strain estimates from calcite grain shapes using Robin's (1977) method. In dry tests these agree well with the experimentally applied strain. In wet tests, however, the assumption that the material remained a continuum is no longer true and the particulate flow accompanying grain deformation causes a stronger grain alignment. In turn, this causes the strain to be overestimated.

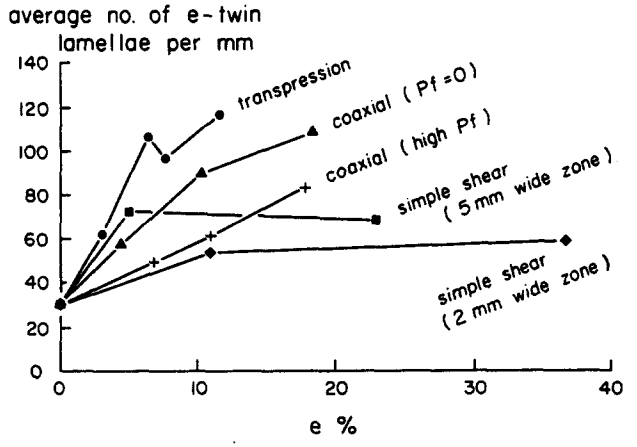

Fig. 22. Intensity of *e*-twin development, shown by the average number of lamellae per mm, in the different kinds of test. Number of lamellae in undeformed material is shown at left, and is derived from the data shown in Fig. 2. The strain (*e*) for each test is given as the equivalent % shortening.

unreliable indicator of the symmetry of bulk deformation under the conditions investigated.

(7) The alignment or *PDO* develops rapidly in pure shear as simulated by the coaxial tests and is already perpendicular to maximum compression at 15% strain (Fig. 18a). However, in shear zones the observations indicate greater complexity. Transpressive shear zones produce an alignment that rotates rapidly towards parallelism with the shear zone walls whereas simple shear produces a feebler alignment inclined to the shear zone walls, similar to theoretical predictions (Fig. 18b). Heterogeneous, '*S–C*' foliation fabrics (cf. Jordan 1987) are not developed at these low shear strains.

(8) The intensity of twinning, recorded by the number of twin lamellae per mm is greatest in transpression and successively less marked in coaxial strain ($P_f = 0$), and simple shear (Fig. 22). The intensity of twinning in simple shear is only marginally greater than that produced by hydrostatic compaction (Fig. 2b indicates the range of twinning intensity for a hydrostatic test). High fluid pressure greatly reduces the incidence of twinning in coaxial triaxial tests at high fluid pressure ($P_f \geq 0.8P_c$).

Acknowledgements—G. Borradaile thanks N.S.E.R.C. (Canada) for generous operating grants (No. A6861) and B.I.L.D. (Ontario) for a capital grant to establish the deformation laboratory. J. McArthur was in receipt of an Ontario Graduate Scholarship during the work. G. Borradaile thanks Stefan Schmid and Mervyn Paterson for helpful correspondence, and Mel Friedman and Ernie Rutter for constructive reviews.

REFERENCES

Borradaile, G. J. 1981. Particulate flow and the formation of cleavage. *Tectonophysics* **72**, 305–321.

Borradaile, G. J. & Alford, C. 1987. Relationships between magnetic susceptibility and strain in laboratory experiments. *Tectonophysics* **133**, 121–135.

Borradaile, G. J. & Alford, C. 1988. Experimental shear zones and magnetic fabrics. *J. Struct. Geol.* **10**, 895–904.

Casey, M., Rutter, E., Schmid, S., Siddans, A. W. B. & Whalley, J. 1978. Texture development in experimentally deformed calcite rocks. In: *Proc. Int. Conf. on the Textures of Materials* (edited by Gottstein, G. & Lucke, K.), Aachen, **5**, 199–210.

Dietrich, D. & Song, H. 1984. Calcite fabrics in a natural shear environment, the Helvetic nappes of Western Switzerland. *J. Struct. Geol.* **6**, 19–32.

Friedman, M. & Conger, F. B. 1964. Dynamic interpretation of calcite twin lamellae in a naturally deformed fossil. *J. Geol.* **72**, 361–368.

Friedman, M. & Higgs, N. G. 1981. Calcite fabrics in experimental shear zones. In: *Mechanical Behaviour of Crustal Rocks. Am. Geophys. Un. Geophys. Monogr.* **24**, 11–27.

Ghosh, S. K. & Ramberg, H. 1976. Reorientation of inclusions by combination of pure and simple shear. *Tectonophysics* **34**, 1–70.

Griggs, D. T., Paterson, M., Heard, H. C. & Turner, F. L. 1960. Annealing recrystallisation in calcite crystals and aggregates. In: *Rock Deformation* (edited by Griggs, D. T. & Handin, J. W.). *Mem. geol. Soc. Am.* **79**, 21–87.

Jordan, P. G. 1987. The deformational behaviour of bimineralic limestone–halite aggregates. *Tectonophysics* **135**, 185–197.

Owens, W. & Rutter, E. H. 1978. Development of magnetic susceptibility anisotropy through crystallographic preferred orientation in experimentally deformed calcite rocks. *Phys. Earth & Planet. Interiors* **16**, 215–222.

Passchier, C. W. & Simpson, C. 1986. Porphyroclast systems as kinematic indicators. *J. Struct. Geol.* **8**, 831–843.

Ramsay, J. G. 1967. *Folding and Fracturing of Rock*. McGraw-Hill, New York.

Robin, P.-Y. 1977. Determination of geological strain using randomly oriented markers of any shape. *Tectonophysics* **42**, T7–T16.

Rutter, E. H. & Rusbridge, M. 1977. The effect of non-coaxial strain paths on the crystallographic preferred orientation development in the experimental deformation of a marble. *Tectonophysics* **39**, 73–86.

Schmid, S. M., Panozzo, R. & Bauer, S. 1987. Simple shear experiments on calcite rocks: rheology and microfabric. *J. Struct. Geol.* **9**, 747–778.

Turner, F. J. 1953. Nature and dynamic interpretation of deformation lamellae in calcite of three marbles. *Am. J. Sci.* **251**, 276–298.

Turner, F. J. & Ch'ih, C. S. 1951. Deformation of Yule marble, Part III: observed fabric changes. *Bull. geol. Soc. Am.* **62**, 887–905.

Turner, F. J., Griggs, D. T., Clark, R. H. & Dixon, R. H. 1956. Deformation of Yule Marble: development of oriented fabrics at 300–500°C. *Bull. geol. Soc. Am.* **67**, 1259–1294.

Wenk, H.-R., Kern, H., van Houtte, P. & Wagner, F. 1986a. Heterogeneous strain in axial deformation of limestone, textural evidence. In: *Mineral and Rock Deformation: Laboratory Studies. Am. Geophys. Un. Geophys. Monogr.* **36**, 287–295.

Wenk, H.-R., Takeshita, T., van Houtte, P. & Wagner, F. 1986b. Plastic anisotropy and texture development in calcite polycrystals. *J. geophys. Res.* **91**, 3861–3869.

Weiss, L. E. & Turner, F. J. 1972. Some observations on translation gliding and kinking in experimentally deformed calcite and dolomite. In: *Flow and Fracture of Rocks* (edited by Heard, H. C., Borg, I. Y., Carter, N. L. & Raleigh, C. B.). *Am. Geophys. Un. Geophys. Monogr.* **16**, 95–107.